

Article

# Influence of Grid Resolution in Modeling of Air Pollution from Open Burning

Duanpen Sirithian<sup>1,2</sup> and Sarawut Thepanondh<sup>1,2,\*</sup>

<sup>1</sup> Department of Sanitary Engineering, Faculty of Public Health, Mahidol University, Bangkok 10400, Thailand; d.sirithian@gmail.com

<sup>2</sup> Center of Excellence on Environmental Health and Toxicology (EHT), Bangkok 10400, Thailand

\* Correspondence: sarawut.the@mahidol.ac.th; Tel.: +66-23-548-540

Academic Editor: Robert W. Talbot

Received: 19 May 2016; Accepted: 14 July 2016; Published: 21 July 2016

**Abstract:** Influences of different computational grid resolutions on modeled ambient benzene concentrations from open burning were assessed in this study. The CALPUFF (California Puff Mesoscale Dispersion Model) was applied to simulate maximum ground level concentration over the modeling domain of  $100 \times 100 \text{ km}^2$ . Meteorological data of the year 2014 was simulated from the Weather Research and Forecasting (WRF) model. Four different grid resolutions were tested including 0.75 km, 1 km, 2 km and 3 km resolutions. Predicted values of the maximum 24-h average concentrations obtained from the finest grid resolution (0.75 km) were set as reference values. In total, there were 1089 receptors used as reference locations for comparison of the results from different computational grid resolutions. Comparative results revealed that the larger the grid resolution, the higher the over-prediction of the results. Nevertheless, it was found that increasing the grid resolution from the finest resolution (0.75 km) to coarser resolutions (1 km, 2 km and 3 km) resulted in reduction of computational time by approximately 66%, 97% and >99% as compared with the reference grid resolution, respectively. Results revealed that the grid resolution of 1 km is the most appropriate resolution with regard to both accuracy of predicted data and acceptable computational time for the model simulation of the open burning source.

**Keywords:** benzene; CALPUFF; grid resolution; maize residue; open burning; Thailand

## 1. Introduction

Agricultural residue burning is classified as an area source of air pollution emitting various kinds of gaseous and particulate pollutants [1,2]. Emissions of these pollutants into the atmosphere can extensively affect environmental quality, visibility, transportation as well as public health [3]. Volatile organic compounds (VOC) have been known to cause both acute and chronic health effects, especially on the respiratory system. Numerous studies indicated that various VOC species are emitted from agriculture residue burning [4–6].

Northern Thailand has experienced air pollution and regional haze problems from burning activities that annually occur during the dry season (January–April). The open burning of maize residues was suggested as one of the major cause of this problem. In 2014, approximately 500,000 hectares of maize are cultivated in the northern region, representing 68% of the total maize acreage in the entire country [7]. Because it is the most convenient and inexpensive method, farmers generally burn their maize residues after harvesting in the dry season for preparing the next crop cycle. This activity leads to a smoke haze episode covering not only the vicinity of burned area but also the northeast region of the country. Results of epidemiological surveillance of health effects in the upper-northern region of Thailand during the haze problem period indicated that significant health

concerns have been related to air pollution, including cardiovascular diseases, respiratory diseases, inflammatory eye diseases and inflammatory skin diseases [8].

Understanding the transport, dispersion and transformation of the compound emitted into the atmosphere is necessary for the development of effective control strategies to reduce emissions and their harmful effects. Air quality modeling is a tool that can be applied to the air quality management system by using various scenarios of related variables (e.g., emission source characteristics, emission rates, climate, population growth, etc.) [9,10]. Because of some limitations of monitoring approach (e.g., locations, instruments and maintenance costs), modeling of air quality is an alternative approach that is widely used for scientific and regulatory purposes [10,11]. Modeled concentrations of air pollutants can provide more spatial and temporal variations than monitoring data. Therefore, they can be very useful in representing the exposure and making a health impact assessment [12,13].

A number of studies have revealed that meteorological conditions and emission rates have greatly influenced the modeled concentrations of any pollutant. However, some studies suggested that results of modeled concentrations were also significantly sensitive to grid resolution [14–18]. Jang et al. [14] used a high-resolution version of the regional acid deposition model (HR-RADM) to simulate ozone ( $O_3$ ) formation at different grid resolutions (20, 40 and 80 km) and found that the use of coarser grid spacing tended to underpredict  $O_3$  maxima because of the of  $O_3$  precursor dilution and to overpredict  $O_3$  minima because of the NO titration effect. They recommended that using the coarser grid spacing did not resolve emission strengths either. Fountoukis et al. [15] examined the impact of grid resolution using the regional three-dimensional chemical transport model (CTM) PMCAMx (Particulate Matter Comprehensive Air quality Model with extensions) over the Northeastern United States with grid resolutions of 36 and 12 km. Results indicated that the use of high resolution decreased the bias for black carbon and organic aerosol concentrations. Shrestha et al. [16] assessed the high-resolution Community Multiscale Air Quality (CMAQ) model at 1, 3 and 9 km grid resolutions in predicting air quality of a highly urbanized region with complex terrain and land-use in Japan. They reported that the finest grid resolution improved the prediction while the coarser resolutions systematically increased the bias of prediction because of higher emission dilution. A better correlation of observations compared to predictions are shown when using fine resolution, and the influence of model resolution was more significant for air quality than for meteorology simulation [17]. Using a coarse grid resolution may produce large discrepancies in the results compared to a fine grid resolution since it cannot capture inhomogeneities in emission rates, meteorology and land cover, while using a fine grid resolution may cause the simulation to be inefficient because it can be considerably limited by calculation time [15,18]. Therefore, model simulation should be performed using the appropriate grid resolution to obtain reliable and acceptable predictions in terms of both accuracy and computational time.

In this study, we assessed the influences of different computational grid resolutions on predicted ambient benzene concentrations from the open burning of maize residue. Due to the sparse distribution of this area source and the need to evaluate dispersion of air pollutants emitted from this activity over a large modeling domain, it is worth studying the influence of grid resolution in modeling air pollution from this open burning source. Therefore, appropriate grid resolution for the CALPUFF (California Puff Mesoscale Dispersion Model) modeling system was determined by taking into consideration model accuracy and computational time. Appropriate grid resolution provides more reliable predicted data for effective applications. It can be applied to further evaluate the contribution of additional emission sources to ambient air quality. The outcome of this study is expected to be of use for assessing public health impacts caused by biomass burning activities. Results of the modeled concentrations at specific receptors can be used for health risk analysis to better understand the public health impacts from maize residue burning in the northern region of Thailand. The reliable results of spatial and temporal air quality help to more accurately define the impacted areas for evaluating appropriate mitigation measures. These are also particularly important for evaluating changes in air quality as a result of implementation of mitigation plans (e.g., agricultural crop substitution, minimizing of area burned, changing burning period).

## 2. Materials and Methods

In this section, the CALPUFF modeling system and its grid system were first described. Next, the processes of modeling domain setting, input parameters and their applications on model simulations to study the effects of computational grid resolutions were presented. Comparative analysis procedures to evaluate the different computational grid resolutions were then described.

### 2.1. CALPUFF Modeling System

The CALPUFF (California Puff Mesoscale Dispersion Model), offered by the U.S. EPA (United States Environmental Protection Agency), is the preferred model for environmental protection and public health studies [19]. The CALPUFF modeling system was applied in several studies, especially for application in areas with complex terrain [11,20–22]. It can be applied for long-range (>50 km) and complex terrains. The CALPUFF modeling system consists of three main components: CALMET (California Puff Mesoscale Diagnostic 3-Dimensional Meteorological Model), CALPUFF (California Puff Mesoscale Dispersion Model) and CALPOST (California Puff Mesoscale Post-Processing Program). CALMET is a meteorological model that generates hourly wind and temperature fields on a three-dimensional gridded modeling domain. CALPUFF is a non-steady-state Lagrangian-Gaussian puff model that uses the CALMET generated wind field and micrometeorological parameters to simulate transport, dispersion, transformation, and deposition for discrete puffs of pollutants emitted from emission sources. CALPUFF calculates hourly concentrations of specified pollutants at specified receptors in a modeling domain. Lastly, CALPOST is the post-processor for CALPUFF, which calculates concentrations and deposition based on the time-averaged pollutant concentration and deposition fluxes that are produced by the CALPUFF [9,23].

CALPUFF uses a three-dimensional Cartesian coordinate reference frame. Three nested grid systems of CALPUFF are meteorological grid, computational grid, and sampling grid. The meteorological grid is the system of grid points at which meteorological parameters such as wind components and mixing heights are defined. The computational grid is where the puffs are released and advected, and it is identical to a subset of the meteorological grid. When the center of a puff is transported outside the computational grid, this puff is eliminated in the next sampling step. In this study, the grid spacing of the computational grid is the same as the meteorological grid. The sampling grid defines the set of gridded receptors and must be equal to or a subset of the computational grid. The grid resolution is a multiple fraction of the resolution of the computational grid [19].

### 2.2. Study Area

Nan, the largest province of maize production in the upper-north region of Thailand in the year 2014, is selected as the study area in this analysis. Total maize cultivation in this province is approximately 1212 km<sup>2</sup>, accounting for about 11% of the provincial area [7]. The modeling domain (Figure 1), is designed for the size of 100 km × 100 km with the reference point position at the NW corner (19°00'10.4"N, 100°17'40.7"E). Four different computational grid resolutions were defined: 0.75 km, 1 km, 2 km and 3 km.

### 2.3. Emission Data

The open burning of maize residues was proposed as one of the major sources of air pollution and regional haze problems during the dry season in the study area. Accordingly, this study is particularly focused on the influence of maize residue burning which affects benzene concentration in the atmosphere. The emission rate of benzene ( $3.54 \times 10^{-7}$  g/s/m<sup>2</sup>) from maize residue burning used for CALPUFF model simulation was calculated based on the emission factor developed from the chamber experimental study. Maize acreages (m<sup>2</sup>) for the year 2014 were taken from the Geographic Information System (GIS) database of the Land Development Department. The distribution of maize

cultivation over the study domain is illustrated in Figure 1 (the center). The red color represents the polygonal area of maize acreage which is interpreted from the satellite images. Because CALPUFF limits the number of sources imported for model simulations ( $\leq 200$  sources), the emission sources were grouped into emission grids. Emission source type was set as a rectangular area. Each emission grid was set to  $5 \text{ km} \times 5 \text{ km}$ . Elevation height of each emission source was set as  $0.8 \text{ m}$  [24]. Areas and coordinates for each rectangular area source were calculated and converted from the shapefiles of GIS database using ArcView GIS version 3.3. In total, there were 195 rectangular area sources used in the model simulation as displayed in Figure 1 (on the right). Each source contained a different emission rate due to different maize areas existing in each emission grid. The averaged emission rate was  $4.91 \times 10^{-8} \text{ g/s/m}^2$  ranging between from  $4.62 \times 10^{-11}$  and  $2.06 \times 10^{-7} \text{ g/s/m}^2$ . For example, an area of maize acreage in source S10 was about  $910,750 \text{ m}^2$ , which accounted for a benzene emission rate of  $0.32 \text{ g/s}$ . The area of each emission grid was equal to  $25 \text{ km}^2$ . Thus, the emission rate of benzene for source S10 was calculated to be  $1.29 \times 10^{-8} \text{ g/s/m}^2$ .

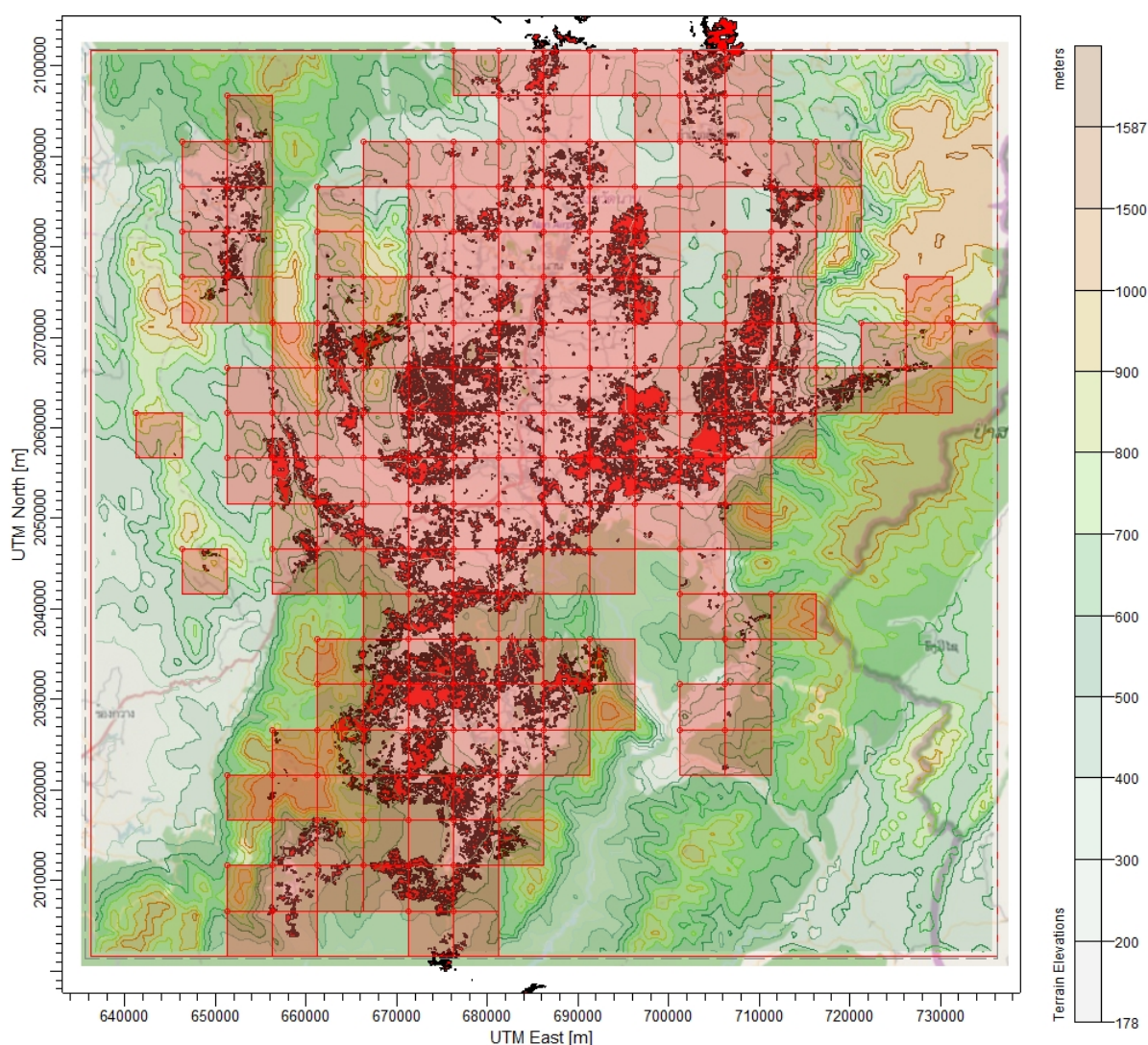


Figure 1. Study domain.

#### 2.4. Model Configuration

The CALMET/CALPUFF model version EPA approved (version 5.8.4) and CALPOST model version EPA approved (version 6.2.2.1) were used for simulations in this study. The Shuttle Radar Topography Mission (SRTM3 ~90 m) was used as terrain database and the Global Land Cover

Characterization (GLCC) for Eurasia optimized for Asia (~1 km) was used as land use database. They were downloaded from WebGIS by CALMET model. Hourly surface and upper meteorological data (3D.dat format) at 12 km resolution for the year 2014 simulated from the Weather Research and Forecasting (WRF) model were used as input meteorological data for CALMET processing. Simulated results of meteorological data from WRF has been intensively validated with the measured data in our previous study [25]. The vertical profile of wind speed and atmospheric temperature measured by the rawinsond system (iMet-1790) in the study area from the year 2009–2011 were used in validation process. Results indicated that predicted data from WRF coincided with those observed data. All simulations were varied only in the computational grid resolutions of the modeling.

The main information of the model setup included: general run control parameters, map projection and grid control parameters, meteorological data options, wind field options and parameters, mixing height, temperature and precipitation parameters, surface and upper air meteorological station parameters, and precipitation station parameters. For general run parameters, the base time zone was set to  $-7$  h. The UTM zone was 47P. The total run length was 2879 h (1 January–30 April 2014). Run type was set to winds and other meteorological variables. In the grid control parameters setting, a rectangular grid (100 km  $\times$  100 km) was defined for all simulations. In the meteorological grid settings, the reference grid coordinate was set as the same position as the modeling domain. Also, the computational grid settings were consistent with the meteorological grid. The number of X grid cells (NX) and Y grid cells (NY) were 133  $\times$  133, 100  $\times$  100, 50  $\times$  50 and 33  $\times$  33 for the computational grid resolutions of 0.75 km, 1 km, 2 km and 3 km, respectively. Besides, 1089 discrete receptors were defined, coinciding with the number of 3 km grid resolution.

In the meteorological data options, it was set to no observation mode. The prognostic meteorological data was used for surface, overwater, upper air data and precipitation. Gridded prognostic wind field from model output was used as an input to the diagnostic wind field model by using winds from the 3D.dat file in the initial guess field. Ten vertical layers with cell face heights in meteorological grid of 0, 20, 40, 80, 160, 320, 640, 1200, 2000, 3000 and 4000 m were used. The minimum radius of influence used in the wind field interpolation ( $R_{MIN}$ ) was set to model default (0.1 km). Radius of influence of terrain features ( $R_{TERRAD}$ ) was set to 50 km. Radius of influence for other parameters (i.e.,  $R_{MAX1}$ ,  $R_{MAX2}$ ,  $R_{MAX3}$ ,  $R_1$  and  $R_2$ ) were not adjusted. Model default values were also used for mixing height, temperature and precipitation parameters, surface and upper air meteorological station parameters, and precipitation station parameters. Since no default dry and wet deposition parameters are available for benzene in CALPUFF, the removal process is not included in the simulation of model. Technical options and computational parameters relating to the CALPUFF dispersion calculation were according to the model defaults.

The dispersion option is used to model the dispersion of pollutants in the atmosphere. SigmaZ and sigmaY are functions of the atmospheric stability class (i.e., a measure of the turbulence in the ambient atmosphere) and of the downwind distance to the receptor. The height of the emission source and the atmospheric turbulence were the important factors affecting the dispersion of pollutants. The more turbulence, the better the degree of dispersion. SigmaZ and sigmaY are optional variables for point source input with the default value of 0.0 m. Since emission source was set to area source, only the initial vertical dispersion coefficient (sigmaZ) of the area source is needed to model input. In the source input data, it was set to 0.8 m, which is the same level as the elevation height of fire from the ground level. In the dispersion coefficient options, Pasquill-Gifford dispersion (PG) coefficients for rural areas were used to compute dispersion coefficients using the default value. The simulation used both sigmaV and sigmaW from profile.dat file to compute sigmaY and sigmaZ.

CALPUFF simulations were performed for four different grid resolutions to predict 24-h average benzene concentrations and their spatial distributions during the burning season of maize residues at corresponding time step. The diurnal variations of emission during 12:00 p.m.–15:00 p.m. were chosen based on the hotspot data. As a result of limited data on the burning period of maize, we assumed the burning period from hotspot data detected from Terra and Aqua MODIS satellites during 1 October

2014–30 April 2015. It was found that approximately 80% of hotspot from the agricultural areas in the study domain occurred during 12:00 p.m.–15:00 p.m. [26]. Results from model simulations were illustrated as the pollution maps of the maximum 24-h average benzene concentrations for different grid resolutions.

### 2.5. Comparative Analysis of Different Computational Grid Resolutions Using Statistical Indicators

The comparative analysis of the results of predicted ambient benzene concentrations obtained from different computational grid resolutions was conducted on the basis of quantitative measures using statistical indicators. Six basic indicators for evaluation of air dispersion models recommended by the U.S. EPA were used in this study, including Fractional Bias (FB), Geometric Mean Bias (MG), Normalized Mean Square Error (NMSE), Geometric Variance (VG), Correlation Coefficient (R) and FAC2 (fraction of predictions within a factor of two of observations), as shown in Equations (1)–(6):

$$FB = \frac{\overline{C_r} - \overline{C_p}}{0.5 \cdot (\overline{C_r} + \overline{C_p})} \quad (1)$$

$$MG = \exp(\overline{\ln C_r} - \overline{\ln C_p}) \quad (2)$$

$$NMSE = \frac{\overline{(C_r - C_p)^2}}{\overline{C_r} \cdot \overline{C_p}} \quad (3)$$

$$VG = \exp\left[\overline{(\ln C_r - \ln C_p)^2}\right] \quad (4)$$

$$R = \frac{(\overline{C_r} - \overline{C_p})(\overline{C_p} - \overline{C_r})}{\sigma_{C_p} \cdot \sigma_{C_r}} \quad (5)$$

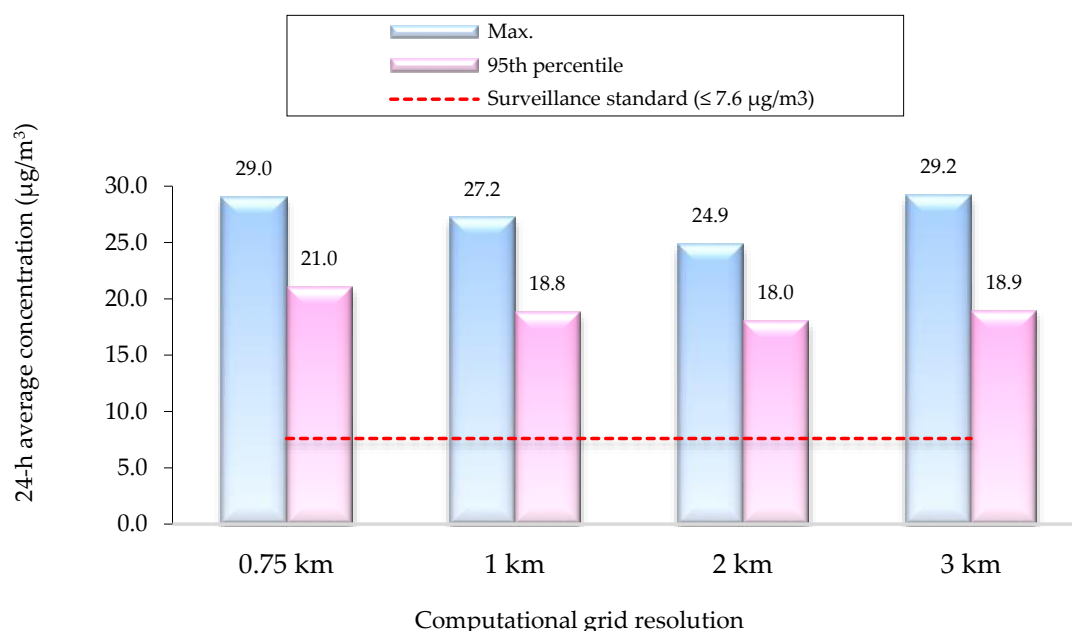
$$FAC2 \text{ (fraction of data satisfy)}, 0.5 \leq \frac{C_p}{C_r} \leq 2 \quad (6)$$

where  $C_r$ —reference concentration,  $C_p$ —predicted concentration,  $\overline{C_r}$ —mean of reference concentrations over the dataset,  $\overline{C_p}$ —mean of predicted concentration over the dataset,  $\sigma_{C_r}$ —standard deviation of reference concentrations over the dataset, and  $\sigma_{C_p}$ —standard deviation of predicted concentrations over the dataset.

Fractional bias (FB) and Geometric Mean Bias (MG) are measures of mean bias and indicate only systematic errors which always underestimate or overestimate the measured values. The fractional bias (FB) is a dimensionless number which is convenient for comparing the results from studies involving different concentration levels. FB is based on a linear scale and the systematic bias which refers to the arithmetic difference between predicted concentration and reference concentration. Geometric Mean Bias (MG) is a measure of mean bias based on a logarithmic scale. Normalized Mean Square Error (NMSE) and Geometric Variance (VG) are measures of scattering and reflect both systematic and unsystematic (random) errors. Correlation Coefficient (R) reflects the linear relationship between two variables. It is insensitive to either an additive or a multiplicative factor. A perfect correlation coefficient is only a necessary, but not sufficient, condition for a perfect model. For example, scatter plot might show generally poor agreement. However, the presence of a good match for a few extreme pairs will greatly improve R. The factor of two (FAC2) is defined as the percentage of the predictions within a factor of two of the observed values (reference values). It is the most robust measure because it is not overly influenced by high and low outlier. Additional details are described elsewhere [27–29]. Predicted values of the maximum 24-h average concentrations obtained from the finest grid resolution (0.75 km) were set as reference values. In total, there were 1089 discrete receptors used as the reference locations for comparison of the modeled results from different computational grid resolutions.

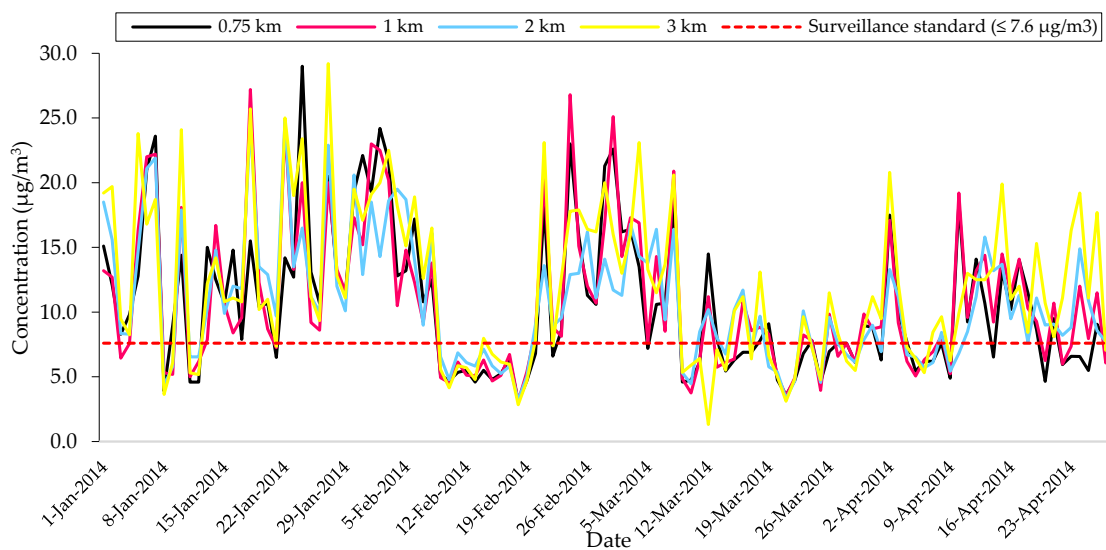
### 3. Results

Figure 2 presents the highest values of the maximum and the 95th percentile of 24-h average concentrations of benzene from four different computational grid resolutions. This value was selected from 1089 receptors located within the entire modeling domains. The highest grid resolution of 0.75 km is used as reference grid resolution. Predicted data from other grid resolutions were used to compare with the values from the reference grid. The highest value of the maximum 24-h average concentrations obtained from the finest grid resolution of 0.75 km (reference grid resolution) was  $29.0 \mu\text{g}/\text{m}^3$ . By using the grid of 3 km, the highest value was slightly higher than the reference value (<1%). On the other hand, the highest values obtained from the grids of 1 km and 2 km were 6% and 14% lower than reference values, respectively. Likewise, the highest values of the 95th percentile of 24-h average concentrations obtained from calculation of all grid resolutions were shown to be similar trends to the highest values of the maximum concentrations. However, there were quite small biases between predicted data and the reference values. Results of the highest values of 24-h average concentrations of benzene in this study exceeded the permissible limit as compared the 95th percentile value with the national ambient surveillance standard for benzene in Thailand ( $\leq 7.6 \mu\text{g}/\text{m}^3$ ).



**Figure 2.** The maximum and the 95th percentile of 24-h average concentrations of benzene from 4 different grid resolutions.

The temporal variations in Figure 3 were plotted using the daily maximum concentration within the study domain. Similar trends of daily maximum concentrations of benzene within the modeling domain during the simulation period (January–April) obtained from four different computational grid resolutions were observed. It should be noted that the constant emission rate was used in the simulation modeling. The 1 km grid resolution better captures temporal variations as compared with the reference grid resolution. Unfortunately, there were a large number of unexpected peak concentrations observed in the 3 km grid resolution. These unexpected peaks in the coarse resolution case could have resulted from the size of the burned area within the emission grid. Since the emission grid used in this analysis was set to  $5 \times 5 \text{ km}^2$ , the burned areas located in the same emission grid that are combined together resulted in different emission rates of each emission grid.



**Figure 3.** Daily maximum values of benzene concentrations from different grid resolutions.

Table 1 compares computational time used in CALMET/CALPUFF simulations for four different grid resolutions. In this study, CALPUFF was simulated using an Intel(R) Core(TM) i5-2320 CPU at 3.00 GHz. It can be seen that using the finer grid resolutions took significantly longer simulated time than the coarser grid resolutions because there were a greater number of grid cells to be simulated. It was found that increasing grid resolution from the finest resolution (0.75 km) to the coarser resolutions (1 km, 2 km and 3 km) resulted in reducing computational time by approximately 66%, 97%, and >99%, respectively.

Predicted values of the maximum 24-h average concentrations at 1089 discrete receptors obtained from the grid of 0.75 km resolution were directly compared with those values from the three remaining computational grid resolutions using aforementioned statistical indicators. Accordingly, three pairs of grid resolutions were classified as P1 (0.75 km vs. 1 km), P2 (0.75 km vs. 2 km) and P3 (0.75 km vs. 3 km). The results of quantified statistic values for different computational grid resolutions relative to the reference values are presented in Table 2.

It was found that the larger the grid resolution, the higher the mean concentration. The FB values were explicitly increased for P1, P2, and P3 when increasing grid resolutions from the finest resolution to the coarse resolutions. The negative values of FB for all pairs indicated the over-prediction of the calculated results. Only the over-predicted result of P1 was within the acceptable limit ( $-0.3 < FB < 0.3$ ) suggested by Chang and Hanna [27]. On the other hand, results of P2 and P3 exceeded the acceptance criteria. Also, the MG value of P1 was acceptable with the perfect comparison result ( $MG = 1$ ). This means that only the result obtained by the grid resolution of 1 km did not differ significantly from the reference grid resolution. In addition, the lowest NMSE and VG values ( $NMSE = 0.7$  and  $VG = 1.1$ ), and the highest R value ( $R = 0.93$ ) were found in P1. FAC2 reflects the percentage of predictions lying within a factor of two of the observations. The results of predicted concentrations for the three different grid resolutions (1 km, 2 km and 3 km) obtained in this study were within a factor of two of the reference value (0.75 km). Therefore, it can be summarized that the use of 1 km resolution produced more accuracy results than the other grid resolutions as compared with the reference grid resolution.

**Table 1.** Comparison of computational time used in CALMET (California Puff Mesoscale Diagnostic 3-Dimensional Meteorological Model)/CALPUFF (California Puff Mesoscale Dispersion Model) simulations for different computational grid resolutions.

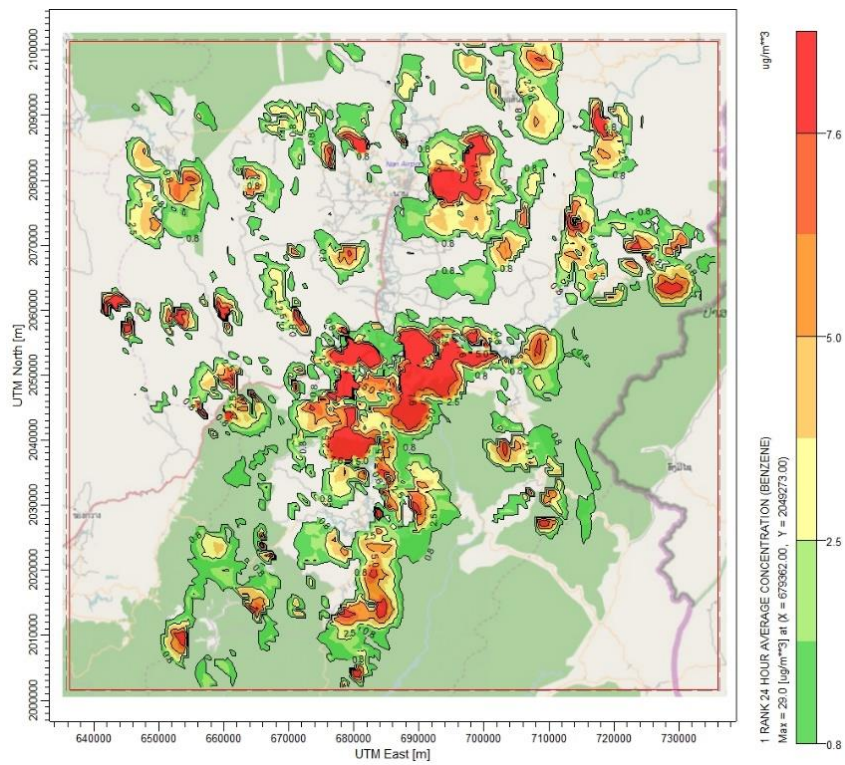
| Model        | Computational Time (min) |            |           |          |
|--------------|--------------------------|------------|-----------|----------|
|              | 0.75 km                  | 1 km       | 2 km      | 3 km     |
| CALMET       | 72                       | 26         | 7         | 2        |
| CALPUFF      | 2284                     | 775        | 60        | 5        |
| <b>Total</b> | <b>2356</b>              | <b>801</b> | <b>67</b> | <b>7</b> |

**Table 2.** Comparison of statistic values for different computational grid resolutions.

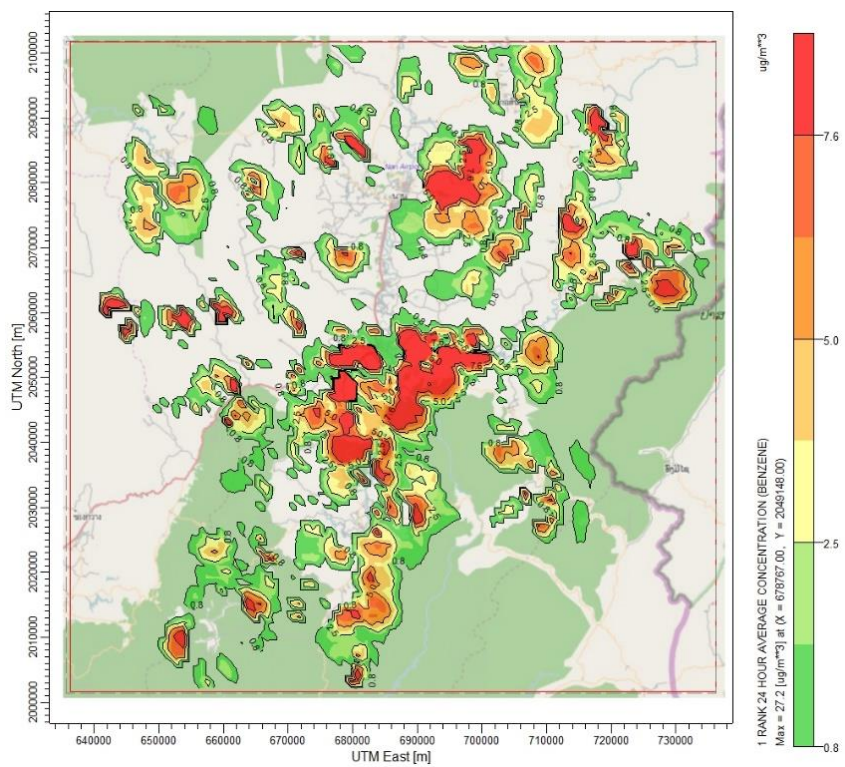
| Statistical Indicator | Computational Grid Resolution |                       |                       | Ideal Value | Acceptable Value [27] |
|-----------------------|-------------------------------|-----------------------|-----------------------|-------------|-----------------------|
|                       | P1 (0.75 km vs. 1 km)         | P2 (0.75 km vs. 2 km) | P3 (0.75 km vs. 3 km) |             |                       |
| $\bar{C}_r$           | 1.1                           | 1.1                   | 1.1                   |             |                       |
| $\bar{C}_p$           | 1.2                           | 1.6                   | 1.8                   |             |                       |
| $\sigma_{C_o}$        | 2.1                           | 2.1                   | 2.1                   |             |                       |
| $\sigma_{C_p}$        | 2.5                           | 3.0                   | 3.6                   |             |                       |
| FB                    | −0.1                          | −0.4                  | −0.5                  | 0.0         | −0.3 < FB < 0.3       |
| MG                    | 1.0                           | 0.7                   | 0.7                   | 1.0         | 0.7 < MG < 1.3        |
| NMSE                  | 0.7                           | 1.4                   | 2.4                   | 0.0         | NMSE < 4.0            |
| VG                    | 1.1                           | 1.5                   | 2.1                   | 1.0         | VG < 1.6              |
| R                     | 0.9                           | 0.9                   | 0.9                   | 1.0         |                       |
| FAC2                  | 1.1                           | 1.7                   | 2.0                   | 1.0         | 0.5 ≤ FAC ≤ 2.0       |

Furthermore, the predicted values from four different computational grid resolutions were analyzed using *t*-test technique. The maximum 24-h average concentrations at 1089 discrete receptors from different computational grid resolutions were compared with the reference values (predicted concentrations using grid spacing of 0.75 km). Results of an independent *t*-test technique at the significance level of 0.05 suggested that there was not significant statistical difference for predicted concentrations at 1 km and 0.75 km grid resolutions (*p*-value = 0.31). However, there were significant statistical differences for predicted concentrations at 2 km or 3 km and 0.75 km grid resolutions (*p*-value < 0.001). Therefore, it can be confirmed that predicted results obtained from 1 km grid resolution are similar to those obtained from the reference grid resolution (0.75 km).

The emission rate was not constantly emitted every hour of every day. Therefore, daily concentration values were used for comparison. The other reason for simulation of daily average concentration in this study is in order to compare results with Thailand's surveillance standard for benzene (≤7.6 μg/m<sup>3</sup>). Figure 4a–d illustrate the spatial distributions of maximum 24-h average concentration of benzene for the grid resolutions of 0.75 km, 1 km, 2 km and 3 km, respectively. It was found that these values occurred at different times and locations, which could be explained by different emissions and meteorological conditions within each sub-grid scale. It can be demonstrated that the use of a grid with a resolution of 1 km showed the smallest discrepancies from the reference grid resolution, while using the coarser grid resolutions produced much larger spatial concentration gradients than the finer grid resolutions. This confirmed the over-prediction of modeled results in our study when a grid resolution becomes coarser. It could be explained by the effect of treatment of the emission grid, as previously described.

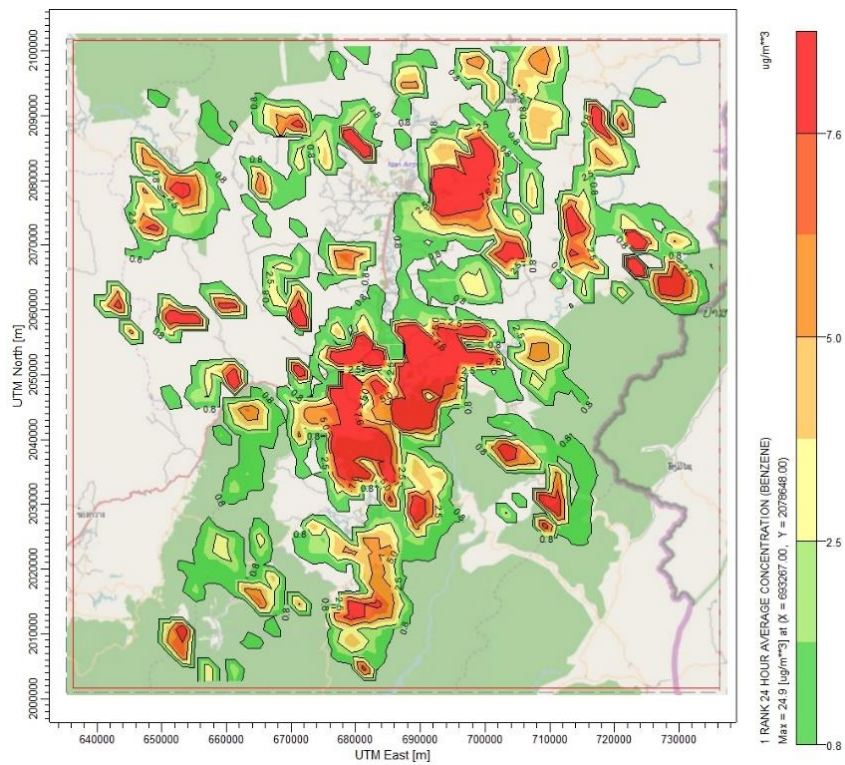


(a)

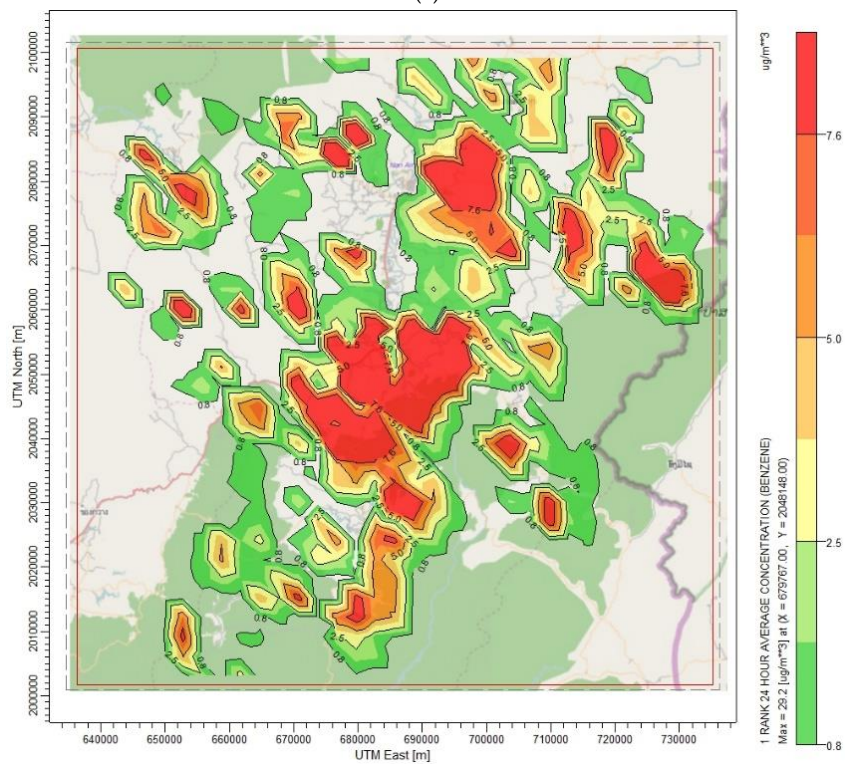


(b)

Figure 4. Cont.



(c)



(d)

**Figure 4.** Spatial distributions of 24-h average concentrations of benzene ( $\mu\text{g}/\text{m}^3$ ) using different grids resolutions: (a) 0.75 km; (b) 1 km; (c) 2 km; and (d) 3 km.

#### 4. Conclusions

The influences of different computational grid resolutions on predicted ambient benzene concentrations from the open burning of maize residue in Nan province, Thailand were assessed in this study. CALPUFF modeling system was simulated to predict maximum 24-h average concentrations over the modeling domain of  $100 \times 100 \text{ km}^2$ . Meteorological data simulated by the WRF model and emission data in the year 2014 were used as input data. Four different computational grid resolutions were tested: 0.75 km, 1 km, 2 km and 3 km. Results showed that the highest values of the maximum 24-h average concentrations obtained by different grid resolutions could be changed by up to 14% from the reference grid resolution (0.75 km) when using a grid resolution of 3 km. Results based on statistical analysis indicated that the use of finer resolutions tend to decrease bias and errors for predicting benzene concentrations. The larger the grid spacing, the higher the predicted results. Statistical analysis indicated that predicted result obtained only by 1 km grid resolution was within an acceptable range for all statistic indicators.

By considering both CALMET and CALPUFF simulations, increasing computational grid resolution from the finest resolution to coarser resolutions (1 km, 2 km and 3 km) resulted in reducing computational time by approximately 66%, 97% and >99% as compared with simulated time used in the reference grid resolution, respectively. Unfortunately, using the coarser grid resolution cannot capture the peak concentrations of benzene as compared to the finest grid resolution. Results of the spatial distributions also indicated that the use of a grid with the resolution of 1 km showed that the smallest discrepancies derived from the reference grid resolution, while using coarser grid resolutions produced much larger spatial concentration gradients than the finer resolutions. Therefore, results from our study indicated that the grid resolution of 1 km is the most appropriate resolution with regards to both accuracy of predicted data and acceptable computational time for the model simulation. It can be considered as an appropriate computational grid resolution for use in modeling air pollution emitted from an area source for regional air quality assessment. This is particularly useful for improvement of the assessment of population-level exposures as well as economic impact analysis which is necessary for effective air quality management.

Emission data used in this study is focused only on maize residue burning. Emissions calculated based on maize acreage in the GIS database may have uncertainties in the magnitude of emission rates and locations. All maize residues were assumed to burn at the same time and the emission rate was constant during 12:00–15:00. Other period times were set as no emissions. The methodology used in this study can be applied in the identification of appropriate computational grid resolution, particularly for the prediction of concentrations from the open burning activities. It should be emphasized that this assessment will be much more accurate when the predicted data are able to be compared with other data, where are available. This process is recommended for further study in this research.

**Acknowledgments:** The authors would like to thank Wanna Laowagul, the Environmental Research and Training Center of Thailand in providing emission data and related parameters for this analysis. Special thanks to the Land Development Department for sharing the Geographic Information System (GIS) database of maize acreage. The Ph.D. scholarship is granted by the Faculty of Public Health, Thammasat University. This study was partially supported for publication by the China Medical Board (CMB), Center of Excellence on Environmental Health and Toxicology (EHT), Faculty of Public Health, Mahidol University, Thailand.

**Author Contributions:** All the authors contributed to the research and experimental design of this study, and to the elaboration of this manuscript. Duanpen Sirithian performed the data collection and analysis, and wrote the first draft of this manuscript; Sarawut Thepanondh supervised the overall research work, provided guidelines for the write-up and editing of the manuscript.

**Conflicts of Interest:** The authors declare no conflict of interest.

## Abbreviations

The following abbreviations are used in this manuscript:

|          |   |
|----------|---|
| VOC      | Volatile Organic Compound   |
| CALMET   | California Puff Mesoscale Diagnostic 3-Dimensional Meteorological Model |
| CALPOST  | California Puff Mesoscale Post-Processing Program                       |
| CALPUFF  | California Puff Mesoscale Dispersion Model                              |
| GIS      | Geographic Information System   |
| U.S. EPA | the United States Environmental Protection Agency                       |
| SRTM     | the Shuttle Radar Topography Mission                                    |
| GLCC     | the Global Land Cover Characterization                                  |
| WRF      | the Weather Research and Forecasting                                    |
| FB       | Fractional Bias Geometric   |
| MG       | Mean Bias   |
| NMSE     | Normalized Mean Square Error  |
| VG       | Geometric Variance  |
| R        | Correlation Coefficient   |
| FAC2     | Fraction of predictions within a factor of two of observations          |
| HR-RADM  | High-resolution version of the regional acid deposition model           |
| CTM      | Chemical Transport Model  |
| PMCAMx   | Particulate Matter Comprehensive Air quality Model with extensions      |
| CMAQ     | Community Multiscale Air Quality  |

## References

- Zhang, H.; Ye, X.; Cheng, T.; Chen, J.; Yang, X.; Wang, L.; Zhang, R.A. Laboratory study of agricultural crop residue combustion in China: Emission factors and emission inventory. *Atmos. Environ.* **2008**, *42*, 8432–8441. [[CrossRef](#)]
- Yuan, B.; Liu, Y.; Shao, M.; Lu, S.; Streets, D.G. Biomass burning contributions to ambient VOCs species at a receptor site in the Pearl River delta (PRD), China. *Environ. Sci. Technol.* **2010**, *44*, 4577–4582. [[CrossRef](#)] [[PubMed](#)]
- Sornpoon, W.; Bonnet, S.; Kasemsap, P.; Prasertsak, P.; Garivait, S. Estimation of emissions from sugarcane field burning in Thailand using bottom-up country-specific activity data. *Atmosphere* **2014**, *5*, 669–685. [[CrossRef](#)]
- Wang, H.; Lou, S.; Huang, C.; Qiao, L.; Tang, X.; Chen, C.; Zeng, L.; Wang, Q.; Zhou, M.; Lu, S.; et al. Source profiles of volatile organic compounds from biomass burning in Yangtze River Delta, China. *J. Aerosol Air Qual. Res.* **2014**, *14*, 818–828. [[CrossRef](#)]
- U.S. Environmental Protection Agency (U.S. EPA). Air Toxics Web Site—Health Effects Notebook for Hazardous Air Pollutants. Available online: <http://www3.epa.gov/ttn/atw/hlthef/hapindex.html> (accessed on 5 April 2015).
- Warneke, C.; Roberts, J.M.; Veres, P.; Gilman, J.; Kuster, W.C.; Burling, I.; Yokelson, R.; de Gouw, J.A. VOC identification and inter-comparison from laboratory biomass burning using PTR-MS and PIT-MS. *Int. J. Mass. Spec.* **2011**, *303*, 6–14. [[CrossRef](#)]
- Office of Agricultural Economics (OAE). Available online: <http://www.oae.go.th/download/prcai/DryCrop/maize.pdf> (accessed on 6 April 2015).
- Department of Disease Control (DDC). Annual Epidemiological Surveillance Report Upper North of Thailand during Haze Problem Period (January–April, 2014). Available online: [http://dpc10.ddc.moph.go.th/epidpc10/download.php?file=17\\_1.pdf&loc=major&type=load](http://dpc10.ddc.moph.go.th/epidpc10/download.php?file=17_1.pdf&loc=major&type=load) (accessed on 11 January 2015).
- U.S. Environmental Protection Agency (U.S. EPA). Preferred/Recommended Models: CALPUFF Modeling System. Available online: [http://www.epa.gov/scram001/dispersion\\_prefrec.htm](http://www.epa.gov/scram001/dispersion_prefrec.htm) (accessed on 8 January 2015).
- Li, Y.; Henze, D.K.; Jack, D.; Kinney, P.L. The influence of air quality model resolution on health impact assessment for fine particulate matter and its components. *Air Qual. Atmos. Health* **2016**, *9*, 51–68. [[CrossRef](#)]
- Ghannam, K.; El-Fadel, M. Emissions characterization and regulatory compliance at an industrial. *Atmos. Environ.* **2013**, *69*, 156–169. [[CrossRef](#)]
- Punger, E.M.; West, J.J. The effect of grid resolution on estimates of the burden of ozone and fine particulate matter on premature mortality in the USA. *Air Qual. Atmos. Health* **2013**, *6*, 563–573. [[CrossRef](#)] [[PubMed](#)]

13. Vaidyanathan, A.; Dimmick, W.F.; Kegler, S.R.; Qualters, J.R. Statistical air quality predictions for public health surveillance: evaluation and generation of county level metrics of PM<sub>2.5</sub> for the environmental public health tracking network. *Int. J. Health Geogr.* **2013**, *12*. [[CrossRef](#)] [[PubMed](#)]
14. Jang, J.-C.C.; Jeffries, H.E.; Byun, D.; Pleim, J.E. Sensitivity of ozone to model grid resolution—I. Application of high-resolution regional acid deposition model. *Atmos. Environ.* **1995**, *29*, 3085–3100. [[CrossRef](#)]
15. Fountoukis, C.; Koraj, D.; Denier van der Gon, H.A.C.; Charalampidis, P.E.; Pilinis, C.; Pandis, S.N. Impact of grid resolution on the predicted fine PM by a regional 3-D chemical transport model. *Atmos. Environ.* **2013**, *68*, 24–32. [[CrossRef](#)]
16. Shrestha, K.L.; Kondo, A.; Kaga, A.; Inoue, Y. High-resolution modeling and evaluation of ozone air quality of Osaka using MM5-CMAQ system. *J. Environ. Sci.* **2009**, *21*, 782–789. [[CrossRef](#)]
17. Tan, J.; Zhang, Y.; Ma, W.; Yu, Q.; Wang, J.; Chen, L. Impact of spatial resolution on air quality simulation: A case study in a highly industrialized area in Shanghai, China. *Atmos. Pollut. Res.* **2015**, *6*, 322–333. [[CrossRef](#)]
18. Garcia-Menendez, F.; Odman, M.T. Adaptive grid use in air quality modeling. *Atmosphere* **2011**, *2*, 484–509. [[CrossRef](#)]
19. Scire, J.S.; Strimaitis, D.G.; Yamartino, R.J. A User's Guide for the CALPUFF Dispersion Model (Version 5.0). Available online: <http://www.src.com> (accessed on 15 December 2014).
20. Jittra, N.; Thepanondh, S. Performance evaluation of AERMOD and CALPUFF air dispersion models in industrial complex area. *Air Soil. Water Res.* **2015**, *8*, 87–95.
21. Thepanondh, S.; Outapa, P.; Saikomol, S. Evaluation of dispersion model performance in predicting SO<sub>2</sub> concentrations from petroleum refinery complex. *Int. J. Geomate* **2016**, *11*, 2129–2135. [[CrossRef](#)]
22. Tartakovsky, D.; Stern, E.; Broday, D.M. Dispersion of TSP and PM<sub>10</sub> emissions from quarries in complex terrain. *Sci. Total. Environ.* **2016**, *542*, 946–954. [[CrossRef](#)] [[PubMed](#)]
23. Lakes Environmental Software. CALPUFF View. Available online: [http://www.weblakes.com/products/calpuff/resources/lakes\\_calpuff\\_view\\_brochure.pdf](http://www.weblakes.com/products/calpuff/resources/lakes_calpuff_view_brochure.pdf) (accessed on 24 January 2015).
24. Huang, X.; Song, Y.; Li, M.; Li, J.; Zhu, T. Harvest season, high polluted season in East China. *Environ. Res. Lett.* **2012**, *7*, 044033. [[CrossRef](#)]
25. Thepanondh, S. *Research Project on Development of Thailand's Assimilative Capacity-Based Air Emission Map: Case of Sulfur Dioxide and Nitrogen Dioxide (Thailand)*; National Research Council of Thailand: Bangkok, Thailand, 2012.
26. Department of National Parks, Wildlife and Plant Conservation (DNP). *Hotspot Information in Thailand*; Ministry of Natural Resources and Environment: Bangkok, Thailand, 2015.
27. Chang, J.C.; Hanna, S.R. *Technical Descriptions and User's Guide for the BOOT Statistical Model Evaluation Software Package, 2nd ed*; Hindawi Publishing Corporation: Cairo, Egypt, 2005.
28. Lee, H.D.; Yoo, J.W.; Kang, M.K.; Kang, J.S.; Jung, J.H.; Oh, K.J. Evaluation of concentrations and source contribution of PM-10 and SO<sub>2</sub> emitted from industrial complexes in Ulsan, Korea: Interfacing of the WRF-CALPUFF modeling tools. *Atmos. Pollut. Res.* **2014**, *5*, 664–676. [[CrossRef](#)]
29. Patryla, L.; Galeriua, D. Statistical Performances Measures—Models Comparison. Available online: <http://www-ns.iaea.org/downloads/rw/projects/emras/emras-two/first-technical-meeting/sixth-working-group-meeting/working-group-presentations/workgroup-7-presentations/presentation-6th-wg7-statistical-performances.pdf> (accessed on 13 May 2015).

